J Mater Sci (2020) 55:2482–2491

Energy materials

MnO_2@NiO nanosheets@nanowires hierarchical structures with enhanced supercapacitive properties

Xiaoli Zhao[1], Xiaoying Liu[2], Fei Li[3,*], and Ming Huang[1,4,*]

[1] College of Material Science and Engineering, Chongqing University, Chongqing 400044, People's Republic of China
[2] Engineering Research Center for Waste Oil Recovery Technology and Equipment of Ministry of Education, College of Environment and Resources, Chongqing Technology and Business University, Chongqing 400067, People's Republic of China
[3] Material Systems for Nanoelectronics, Technische Universität Chemnitz, 09107 Chemnitz, Germany
[4] School of Materials Science and Engineering, Ulsan National Institute of Science and Technology (UNIST), Ulsan 44919, Republic of Korea

Received: 12 August 2019
Accepted: 8 October 2019
Published online: 11 October 2019

ABSTRACT

Transitional metal oxides are demonstrated as promising candidates for pseudocapacitive electrode materials for use in high-performance supercapacitors. Here, we report a rational design of the MnO_2@NiO nanosheets@nanowires hybrid structure. The as-prepared hierarchical structure shows highly uniformity and interconnection between ultrathin MnO_2 nanosheets and NiO nanowires. The well-designed MnO_2@NiO is directly used as binder-free electrode and exhibits a high specific capacitance (374.6 F g^{-1} at a current density of 0.25 A g^{-1}; areal capacitance of 1.3 F cm^{-2}), good rate capability, and excellent cycling stability (92.7% capacitance retention after 5000 charge/discharge cycles). An asymmetric supercapacitor (ASC) is assembled using the MnO_2@NiO as the positive electrode and activated microwave exfoliated graphite oxide as the negative electrode. The assembled ASC shows excellent electrochemical performance with an energy density of 15.4 W kg^{-1} and a maximum power density of 9360 W kg^{-1}. These analytical and experimental results clearly indicate the advantages of multicomponent hierarchical core–shell structure for engineering high-performance electrochemical capacitors.

Introduction

In the past decade, supercapacitors (SCs) have been extensively studied and recognized as the most potential candidate for promising and high-quality energy storage system because of their fascinating features which include excellent power density, good rate capability, long cycle life, and safe operation [1–6]. Up to now, supercapacitors have been mainly divided into two kinds due to their charge/discharge behavior and/or charge storage mechanisms: electric double-layer capacitors (EDLCs) and the pseudocapacitors [7–9]. EDLCs always use high surface area

Address correspondence to E-mail: f.li@ifw-dresden.de; huang@unist.ac.kr; xiaoming.huang694@gmail.com

https://doi.org/10.1007/s10853-019-04112-4

carbon-based materials (graphene, CNTs, porous carbon) which can achieve the charge storage at the interface between electrode and electrolyte. However, the low capacity and energy density of the EDLCs are yet to be improved, hindering the potential application for the high-performance energy storage. In contrast to EDLCs, pseudocapacitors can store the charge via redox reactions, intercalation and/or electrosorption, resulting in much higher electrochemical pseudocapacitance. Pseudocapacitor is mostly based on metal oxides/hydroxides due to their multiple oxidation chemical states which are favorable for larger charge storage in the charge/discharge process.

Up to now, numerous studies have been focused on various metal oxides for high-performance pseudocapacitor electrodes, such as RuO_2, Co_3O_4, NiO, CuO and MnO_2 [10–14]. Among these candidates for high-performance electrodes, MnO_2 was believed to the most promising candidate for the fabrication of electrodes due to its high theoretical specific capacitance (close to 1400 F g^{-1}), abundant resources, and environmental compatibility [15–18]. There have been lots of works devoted to explore various structures/morphologies and MnO_2-based hybrid/composite materials for high-performance supercapacitors [19–24]. Nevertheless, a literature survey has indicated that the state-of-the-art capacitance of pure MnO_2 electrodes is still far below the theoretical value. One potential strategy to further improve the capacity is to integrate two or more active materials with high redox electroactivity into one ordered nanostructure. Adopting this idea, more space or active surface/interface of the hybrid/composite structure would be created for the enhanced energy storage and the synergistic effect between different active materials can be utilized. It is noteworthy that NiO could be a promising candidate to integrate with MnO_2 because of its excellent reversible redox activity, large theoretical capacitance (around 2573 F g^{-1}), environment friendly nature and natural abundance [25].

In this paper, we reported the preparation of MnO_2@NiO nanosheets@nanowires hierarchical structures and their use in supercapacitor electrodes. With the aid of electron microscopy (SEM), energy-dispersive X-ray spectroscopy (EDS) and transmission electron microscopy (TEM), we found that the NiO nanowires are uniformly deposited on the surface of MnO_2 nanosheets to form a hierarchical nanosheet@nanowire structure. With the smart design for this integrated structure, a synergistic effect has been indicated: MnO_2 nanosheet arrays provide a robust and porous scaffold for the further deposition of NiO nanowires to avoid the aggregation, while the further deposited NiO nanowires could highly increase the pseudocapacitance. When the MnO_2@NiO was used as a binder-free electrode, it exhibits a large specific capacitance (374.6 F g^{-1} at a current density of 0.25 A g^{-1}) and good cycling stability (92.7% capacitance retention with respect to the initial capacitance before cycling test). The strategy for engineering of MnO_2@NiO nanosheets@nanowires hierarchical electrode with high performance can stimulate more interest in the exploration for hierarchical MnO_2-based composites for use as multi-functional active materials in various fields.

Materials and methods

Synthesis of MnO_2 nanosheets on nickel foam

MnO_2 nanosheet on nickel foam was prepared through a one-step hydrothermal reaction. Before the hydrothermal reaction, Ni foam was cleaned in 3 M HCl aqueous solution to remove the surface NiO layer and ultrasound-treated with deionized water (DI water) and ethanol by ultrasonication for 20 min. The treated Ni foam was put into an autoclave followed by adding 30 mL of 0.05 M $KMnO_4$ solution for hydrothermal reaction (the autoclave was kept at 160 °C for 24 h). Upon the cooling of the autoclave, the sample was taken out and cleaned by ultrasonication in DI water and ethanol for 30 min and finally dried in an oven at 80 °C. The loading mass of the MnO_2 sheets on Ni foam is calculated to be around 1.8 mg cm^{-2}.

Preparation of MnO_2@NiO nanosheets@nanowires hierarchical structures

Before the deposition of NiO nanowires onto MnO_2 nanosheets, a solution (35 mL) contains 1 mmol $Ni(NO_3)_2{\cdot}6H_2O$ and 2 mmol $CO(NH_2)_2$ was prepared. And then the MnO_2 deposited Ni foam was put into the as-prepared solution and transferred to

the autoclave for a further hydrothermal reaction (kept in an oven set at 120 °C for 12 h). The sample was washed with DI water and ethanol and dried in an oven (set at 80 °C). After washing and drying, the sample was annealed at 300 °C for 2 h to get the MnO_2@NiO nanosheets@nanowires hierarchical structures on Ni foam (the areal density of the MnO_2@NiO composite is around 3.5 mg cm^{-2}).

Characterization and electrochemical measurements

The detailed materials characterization and electrochemical tests of the as-prepared samples are shown in the experimental section in Supporting Information.

Results and discussion

The procedure for fabrication of MnO_2@NiO nanosheets@nanowires hierarchical structure is shown in Fig. 1. In the first step, highly uniform MnO_2 nanosheets were first grown on Ni foam by a simple hydrothermal reaction using $KMnO_4$ as precursor. The bare Ni foam and MnO_2 nanosheets-coated Ni foam can be easily distinguished from the SEM images shown in Figs. S1 and 2a, b. Typically, the bare Ni foam shows a macroporous structure with a smooth surface. The XRD pattern of the Ni foam only shows the XRD peaks from pure Ni after acid-treatment (inset in Fig. S1). After the hydrothermal reaction, a large arrays of MnO_2 nanosheets were uniformly coated on the surface of Ni foam (Fig. 2a, b), resulting in a highly porous and interconnected structure, which can facilitate the fast transport of electrolyte ions during the electrochemical reactions. The thickness of the MnO_2 nanosheets layer was found to be around 1.6 μm in Fig. S2b. The MnO_2 nanosheets is found to be very robust and stable even after an ultrasonication treatment for more than 30 min before the SEM measurement, indicating its potential use for large-scale production. In the second step, NiO nanowires were obtained by a second hydrothermal reaction together with a further calcination process in air. SEM images of the MnO_2@NiO nanosheets@nanowires are shown in Fig. 2c, d which indicates a highly uniform and porous structure. The wall of the MnO_2 nanosheets was uniformly coated with many NiO nanowires, forming a feather-like structure. This feather-like porous structure was believed to be highly accessible to electrolyte ions and robust for use as electrodes. After deposition of NiO nanowires, the thickness of the MnO_2@NiO nanosheets@nanowires composite was increased to around 2.3 μm (Fig. S3), indicating a greater loading mass of the active materials which would be benefit for larger output of the capacitor device.

The microstructure of the MnO_2@NiO nanosheets@nanowires was further verified using TEM. We first check the HRTEM image of the MnO_2 nanosheets, and the result is shown in Fig. S4. It was

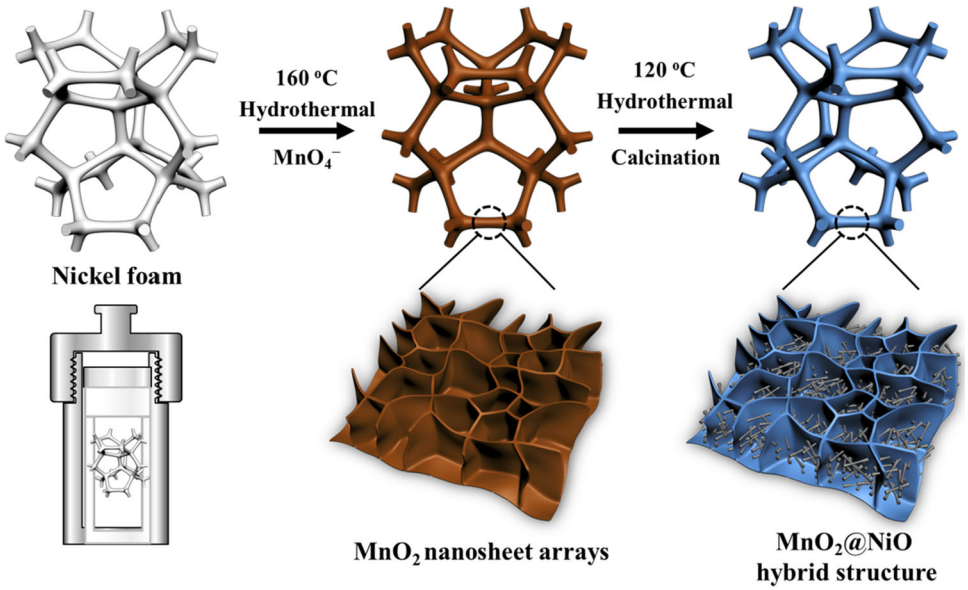

Figure 1 Schematic illustration of the synthesis of MnO_2@NiO nanosheets@nanowires hierarchical structure.

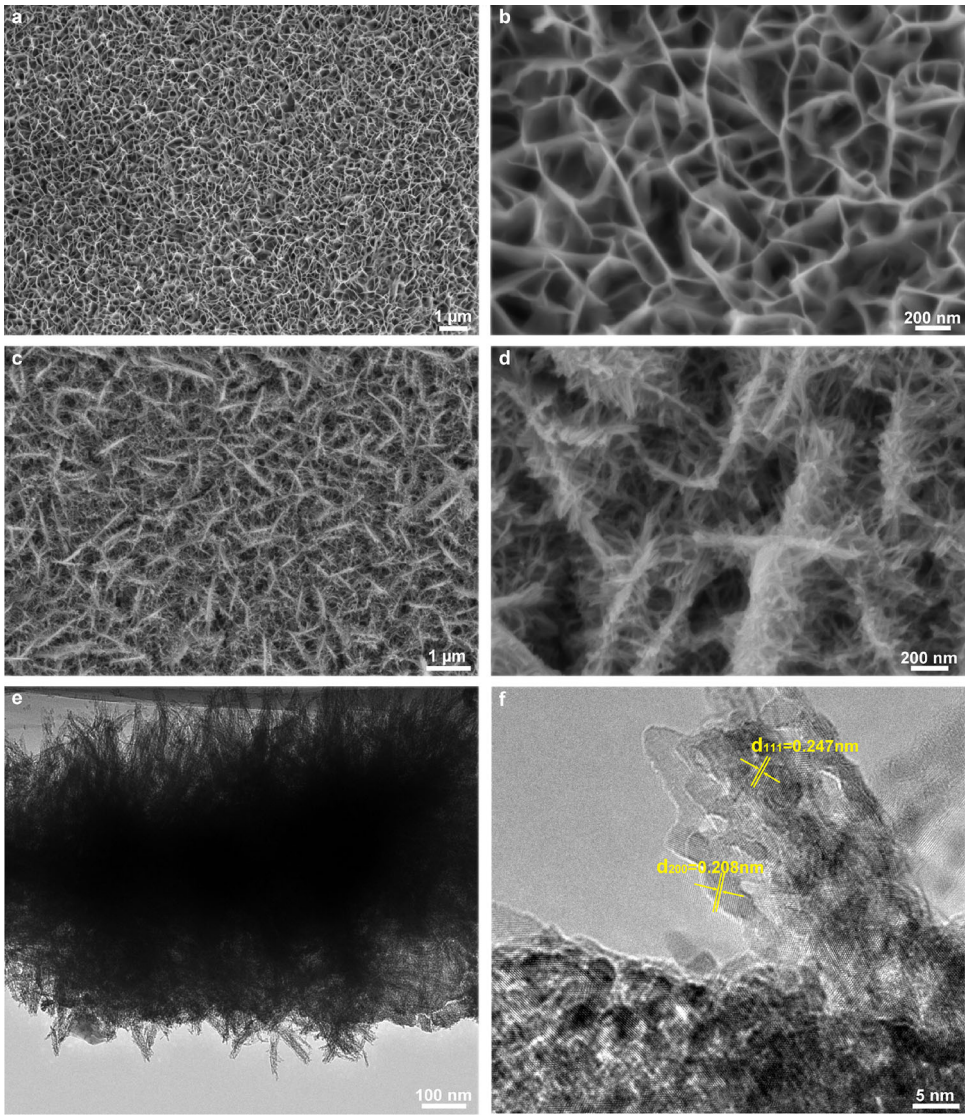

Figure 2 **a**, **b** SEM images of MnO_2 sheets on Ni foam. **c**, **d** SEM images of MnO_2@NiO nanosheets@nanowires hierarchical structure on Ni foam. **e**, **f** TEM images of MnO_2@NiO nanosheets@nanowires hierarchical structure.

clearly found that the average thickness of the MnO_2 nanosheets is around 5–10 nm. A clear lattice spacing of 0.67 nm shown in Fig. S4b was corresponded to the interplanar spacing of the (001) plane of birnessite-type MnO_2. TEM image of the hybrid MnO_2@NiO nanosheets@nanowires structure is shown in Fig. 2e in which the wall of MnO_2 nanosheets was uniformly coated with tiny and porous NiO nanowires. The diameter of the NiO nanowires was estimated to be around 15–20 nm from the HRTEM image (Fig. 2f). The two lattice spacing of 0.247 and 0.208 nm in the NiO nanowire were corresponded to the (111) and (200) interplanar spacing of bunsenite NiO (JCPDS card No. 47-1049). These TEM results further indicate the core–shell structure of the MnO_2@NiO nanosheets@nanowires. The crystal phase of the MnO_2 nanosheets and MnO_2@NiO nanosheets@nanowires was determined by powder XRD (Fig. 3a). The diffraction peaks of the MnO_2 nanosheets were well matched with the standard peaks from birnessite-type MnO_2 (JCPDS card No. 80-1098) [26], except the three strong diffraction peaks from the Ni substrate. After the deposition of NiO nanowires, three new emerged peaks at 37.2°, 43.2°, and 62.8° were indexed to the (111), (200), and (220) planes of bunsenite NiO (JCPDS card No. 47-1049) [12]. Figure S5 shows the XRD pattern of the precursor coated on MnO_2/Ni substrate (after second hydrothermal reaction but before the calcination process to obtain NiO). Except the peaks from MnO_2 and Ni foam, the other diffractions peaks are in good agreement with the standard peaks from a nickel

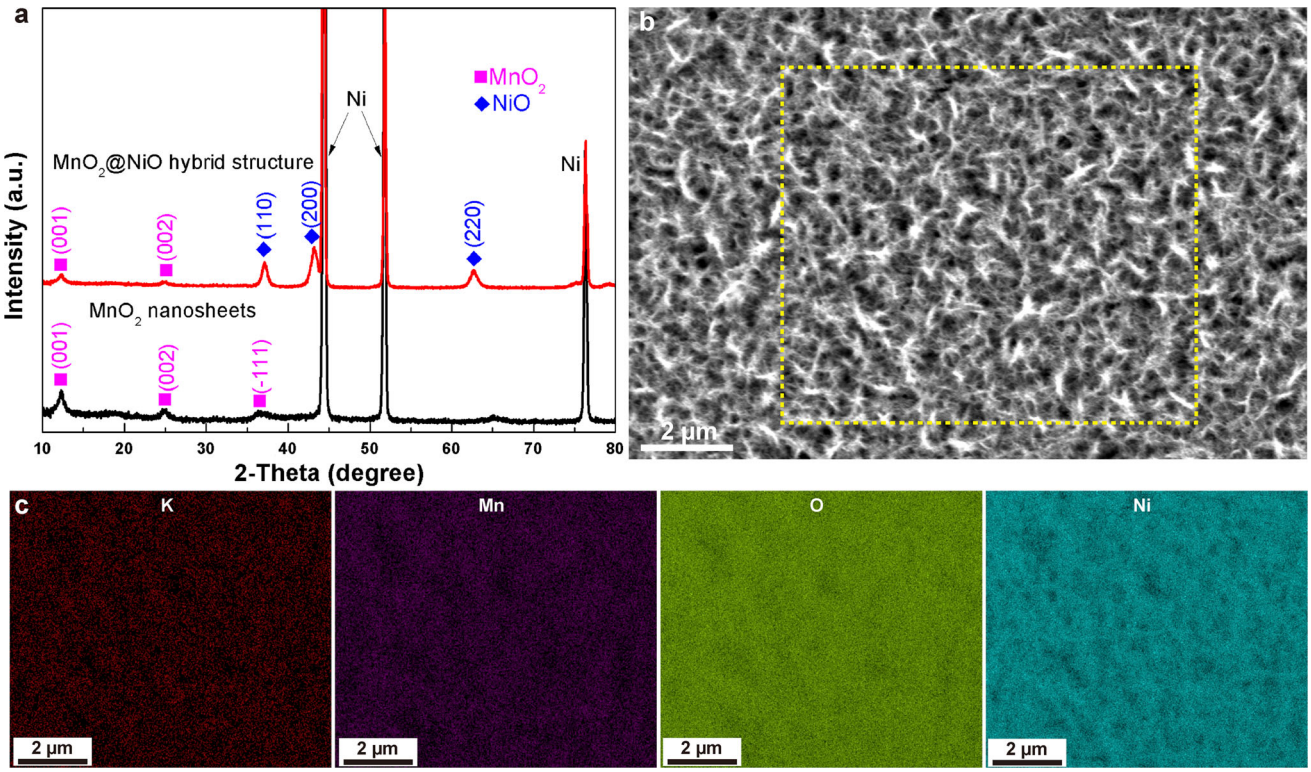

Figure 3 **a** XRD patterns of MnO_2 nanosheets and MnO_2@NiO nanosheets@nanowires hierarchical structure on Ni foam. **b**, **c** SEM image and EDS mapping of MnO_2@NiO nanosheets@nanowires hierarchical structure on Ni foam.

hydroxide carbonate ($Ni_2(OH)_2CO_3$; JCPDS, No. 35-0501). In addition, the EDS mapping (Fig. 3b, c) of the MnO_2@NiO nanosheets@nanowires was also performed to indicate the uniformity and purity (the EDS mapping of MnO_2 nanosheets is shown in Fig. S6). The EDS mapping shows homogenous distribution of K, Mn, O, and Ni, further indicating the successful deposition of NiO on the MnO_2 nanosheets to form the MnO_2@NiO nanosheets@nanowires core–shell structure. N_2 adsorption–desorption measurements were performed to study the surface area and porosity of the MnO_2@NiO nanosheets@nanowires composite (Fig. S7). The results indicate that the MnO_2@NiO has a BET surface area of 47.8 $m^2\ g^{-1}$ with a pore volume of 0.21 $cm^3\ g^{-1}$. The pore size distribution obtained from the desorption branch by the Barrett–Joyner–Halenda (BJH) method indicates an average pore size of $\sim$ 15.8 nm, suggesting a mesoporous structure.

X-ray photoelectron spectroscopy (XPS) was used to further check the surface compositions and chemical state of the MnO_2@NiO composite. As shown in Fig. 4a, the core-level Ni2*p* spectrum shows a multiplet-split Ni2$p_{3/2}$ peak, a multiplet-split Ni2$p_{1/2}$ peak and two corresponding shake-up-satellite peaks, suggesting the existence of NiO [27, 28]. The Mn2*p* spectrum (Fig. 4b) exhibits two main peaks located at 642.4 eV (Mn2$p_{3/2}$) and 654.2 eV (Mn2$p_{1/2}$) with a spin-energy separation of 11.8 eV, indicating the chemical state of Mn^{4+} in MnO_2 [29]. In addition, the Mn3*s* spectrum (Fig. 4c) has two multiplet-split components which can be also used to distinguish Mn oxidation states. The spin-energy splitting (ΔE) of 4.7 eV further suggests the oxidation state of Mn^{4+} in MnO_2@NiO composite [30]. The O1*s* spectrum shown in Fig. 4d exhibits two main peaks at 529.9 and 531.7 eV which are attributed to metal–oxygen bonds (Ni/Mn–O) and metal hydroxide (Ni/Mn–OH), respectively. The very tiny peak located at around 533.3 eV is due to the small amount of absorbed water on the surface of MnO_2@NiO composite. The K2*p* spectrum is also shown in Fig. S8, which is matching with the EDS result. Based on the SEM, EDS, XRD, TEM and XPS results, the hierarchical MnO_2@NiO nanosheets@nanowires composite that tightly connected with the Ni foam collector has been successfully achieved,

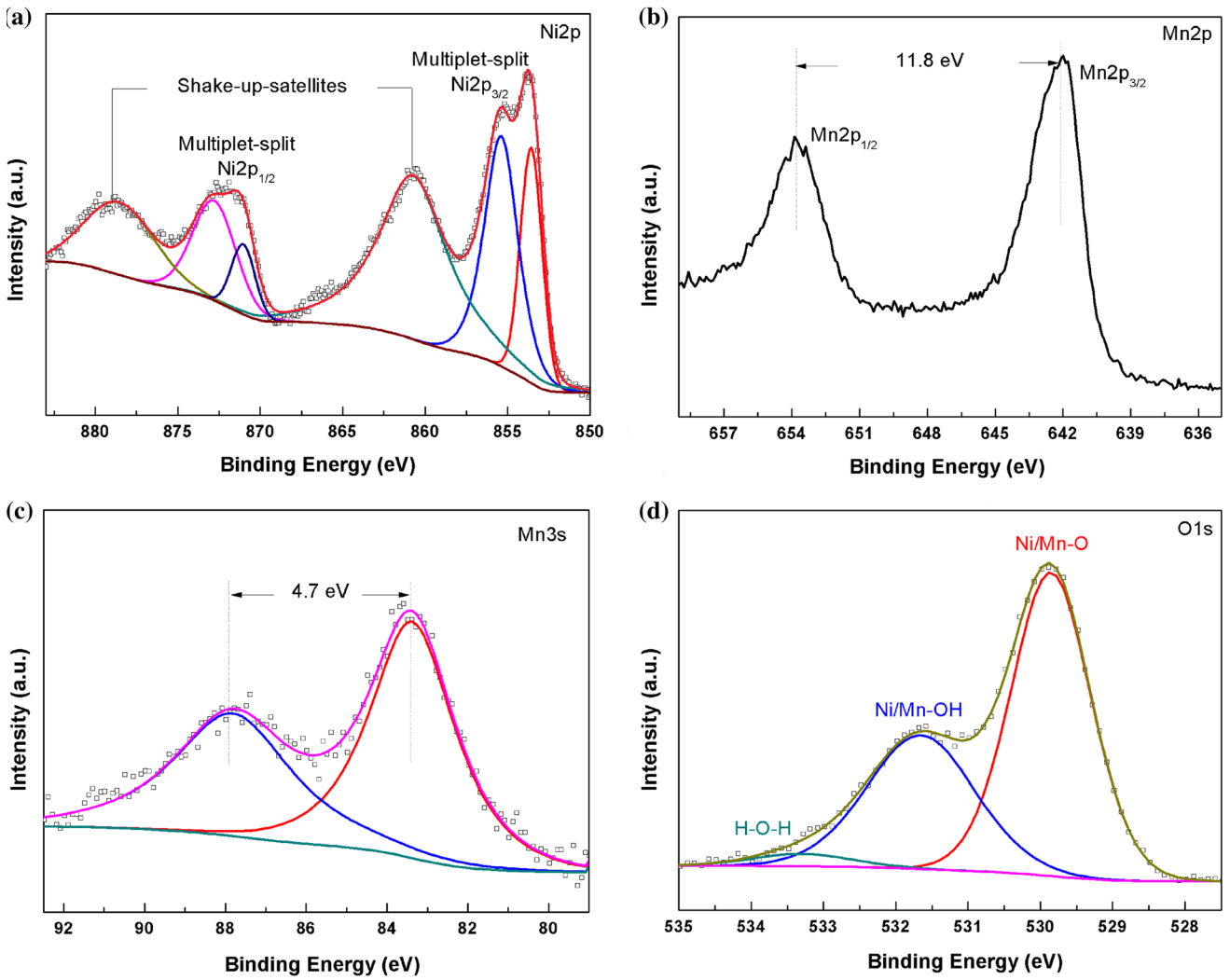

Figure 4 XPS spectra of **a** Ni2*p*, **b** Mn2*p*, **c** Mn3*s* and **d** O1*s* for MnO_2@NiO nanosheets@nanowires composites.

which is crucial for fabricating highly conductive and high-performance binder-free electrodes.

To evaluate the capacitive property, the MnO_2@NiO nanosheets@nanowires on nickel foam substrate was utilized as a binder-free electrode and tested. We first measured the CV curves of the MnO_2@NiO electrode at different scan, and the result is shown in Fig. 5a. The asymmetrical redox peaks clearly indicate the pseudocapacitive nature of the MnO_2@NiO electrode. It was found that the current changes significantly upon the increase in the scan rates, but the potentials of the reversible redox peaks show slight changes, suggesting an excellent reversibility of the electrodes. Thus, the charge storage mechanism of MnO_2@NiO active material is mostly attributed to the pseudocapacitance from reversible redox (Faradaic) reactions. We further measure the charge/discharge response of the electrode, and the result is shown in Fig. 5b. The nonlinear GCD curves further indicate the pseudocapacitive nature of the MnO_2@NiO electrode, which is matched with the results we observed in CV test. As calculated at a current density of 0.25 A g^{-1} from the GCD curve, the MnO_2@NiO electrode possesses a large specific capacitance of 374.6 F g^{-1} (areal capacitance of 1.3 F cm^{-2}). The specific capacitance of MnO_2@NiO composite electrode is larger than that of MnO_2@Ni foam (308.4 F g^{-1}) and NiO@Ni foam electrodes (257.3 F g^{-1}), suggesting a synergetic effect between these two components (detailed result of the electrochemical test of MnO_2@Ni foam and NiO@Ni foam electrodes is shown in Fig. S9). In addition, we have measured the charge/discharge curves at various current densities and extracted the

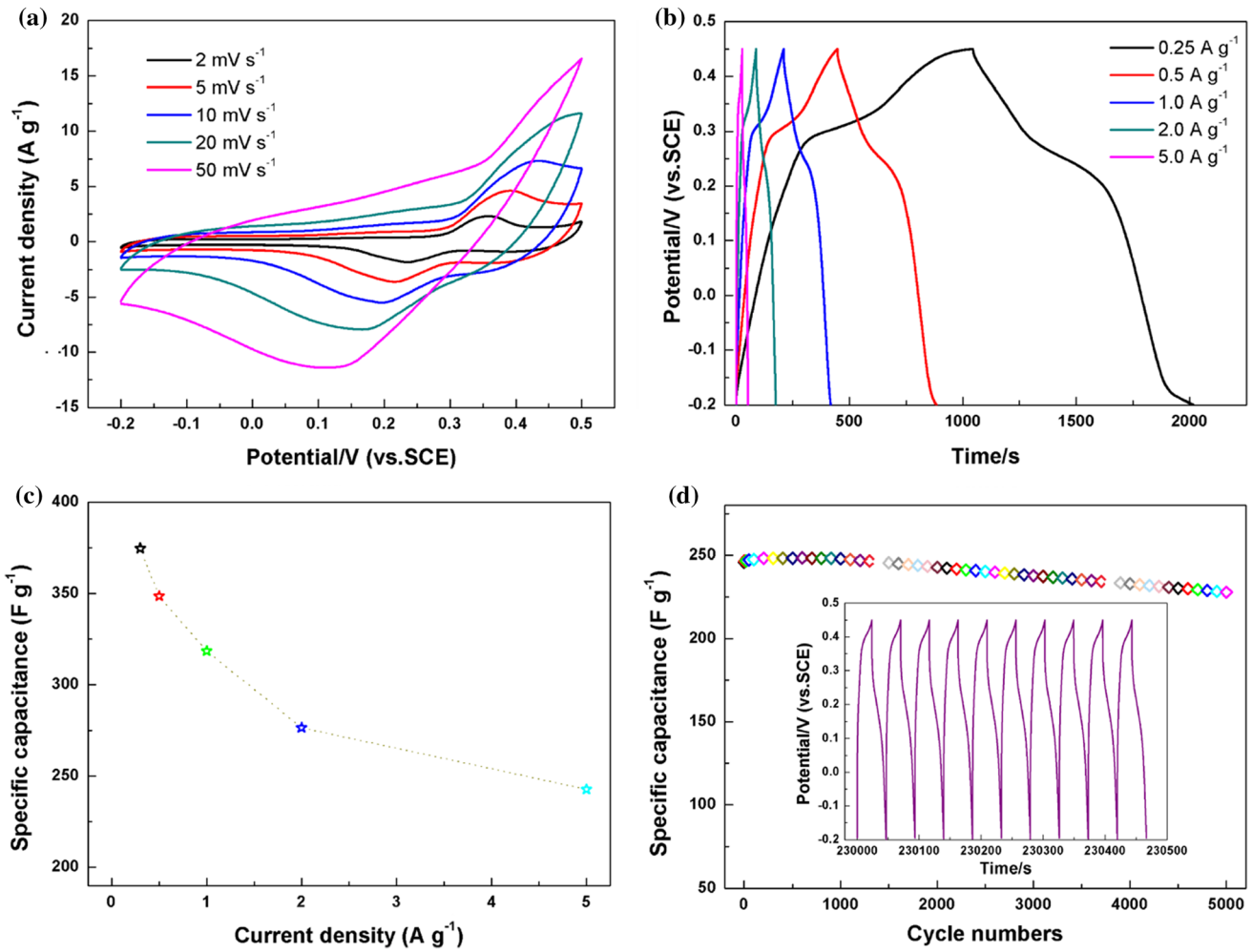

Figure 5 **a** Cyclic voltammograms of MnO_2@NiO nanosheets@nanowires electrode in 1 M KOH aqueous electrolyte. **b** Charge/discharge curves at different current densities. **c** Specific capacitance measured at different current densities. **d** Cycling performance of the electrode. The inset shows the charge/discharge curves of the last 10 cycles of the electrode.

corresponding specific capacitances (Fig. 5c). It is clear that the specific capacitance of the MnO_2@NiO electrode shows a retention of 64.8% with a 20-time increase in the current density (up to 5 A g^{-1}), suggesting a good rate performance. The good electrochemical performance was due to the good electrical contact between MnO_2@NiO nanosheets@nanowires with the Ni foam collector and also the large surface area of the porous nanowires-on-nanosheets structure. The cycling stability of the hierarchical MnO_2@NiO electrode was further evaluated via charge/discharge tests for 5000 cycles. The capacitance retains approximately 92.7% of its initial value after cycling test, suggesting a good cycling performance. In addition, we did not observe any change of the GCD curves after 5000 cycles (inset in Fig. 5d), further indicating the high stability of our hierarchical MnO_2@NiO electrode.

To show the potential use of the MnO_2@NiO nanosheets@nanowires composite as electrode material for high-performance capacitor device, we have fabricated an asymmetric supercapacitor (ASC) device using MnO_2@NiO and activated microwave exfoliated graphite oxide (MEGO) as the positive and negative electrodes, respectively. CV curves of the ASC were first recorded at various pre-set voltage windows to explore the optimal potential windows four device (Fig. 6a). It is clear that the ASC could reach an optimal window up to 1.6 V without significant polarization. This large potential window will be benefit for increasing the energy density at a given specific capacitance. We further measured the charge/discharge response of the electrode (Fig. 6b)

at several pre-set current densities. All the charge/discharge curves show similar shapes and behaviors, indicating a good rate capability which is crucial for high-power supercapacitors. We have thus calculated the specific capacitance of the total device (considering the whole weight of the cathode and anode (i.e., mass of MnO_2@NiO + MEGO)) from the discharge branch. The calculated capacitance of the ASC is 43.4 F g^{-1} at a pre-set current density (0.25 A g^{-1}). In addition, the specific capacitances of the ASC at a series of current densities are shown in Fig. 6c. The good rate capability can be ascribed to the fast and reversible electrochemical reactions during the charge/discharge process. As is known to all that the high-quality supercapacitors should own both high energy density and power density, we have thus recorded the Ragone plot of the MnO_2@NiO//MEGO capacitor (Fig. 6d). The ASC device shows a good gravimetric energy density (15.4 W kg^{-1}) and a large power density (9360 W kg^{-1}), which are superior to those of MnO_2-based and NiO-based ASC devices [26, 29, 31–34]. These fascinating capacitive performances might be due to the hierarchical and porous nanowires-on-nanosheets structure and the synergistic effect of these two components. The results indicate that the as-prepared MnO_2@NiO nanosheets@nanowires composite on Ni foam could find use in bind-free electrode materials for high-performance pseudocapacitors.

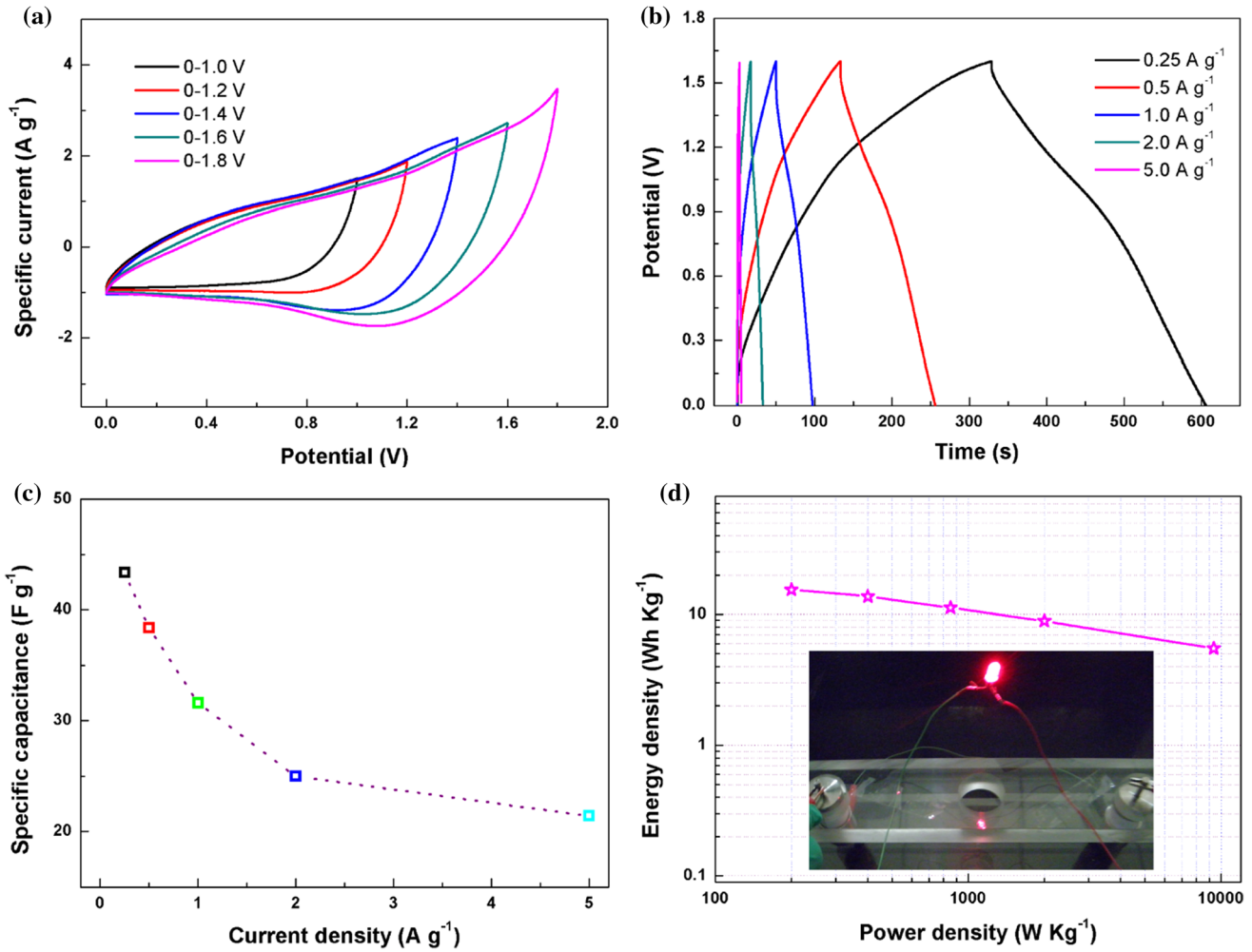

Figure 6 **a** Cyclic voltammograms of MnO_2@NiO//MEGO ASC device measured at different potential windows at a scan rate of 50 mV s^{-1}. **b** Galvanostatic charge/discharge curves recorded at different current densities. **c** Specific capacitances as a function of current densities. **d** Ragone plot of the assembled ASC device. The inset shows that a red-light-emitting diode (LED) was lighted by the charged ASC device.

Conclusions

We have synthesized uniform MnO_2@NiO nanosheets@nanowires hierarchical structures and used them as binder-free electrodes for supercapacitors. Various measurements were conducted to investigate the hierarchical core–shell nanostructure, and it was found to be of very high uniformity. With the rational design of the hierarchical and porous structure and the synergistic effect of different components, the as-prepared MnO_2@NiO shows a good specific capacitance (374.6 F g^{-1} at a current density of 0.25 A g^{-1}; areal capacitance of 1.3 F cm^{-2}) with an outstanding cycling performance (a 92.7% capacitance retention after 5000 charge/discharge cycles). In addition, a large-potential-window ASC device with successfully fabricated using MnO_2@NiO as cathode material and MEGO as anode material shows promising energy and power densities. Our work here proposed a simple but effective strategy for the low-cost and massive preparation of hierarchical and porous composites for use as high-quality and stable supercapacitor electrodes.

Acknowledgements

The financial support funded by Chongqing Special Postdoctoral Science Foundation (XmT2018043) was highly appreciated. FL acknowledges the support and funding from China Scholarship Council (CSC).

Compliance with ethical standards

Conflict of interest All authors listed have declared that they have no conflict of interest.

Electronic supplementary material: The online version of this article (https://doi.org/10.1007/s10853-019-04112-4) contains supplementary material, which is available to authorized users.

References

[1] Miller JR, Simon P (2008) Electrochemical capacitors for energy management. Science 321:651–652

[2] Wang G, Zhang L, Zhang J (2012) A review of electrode materials for electrochemical supercapacitors. Chem Soc Rev 41:797–828

[3] Huang M, Li F, Dong F, Zhang YX, Zhang LL (2015) MnO_2-based nanostructures for high-performance supercapacitors. J Mater Chem A 3:21380–21423

[4] Wang J, Li F, Zhu F, Schmidt OG (2018) Recent progress in micro-supercapacitor design, integration, and functionalization. Small Methods 3:1800367

[5] Yu Z, Tetard L, Zhai L, Thomas J (2015) Supercapacitor electrode materials: nanostructures from 0 to 3 dimensions. Energ Environ Sci 8:702–730

[6] Ji J, Zhang LL, Ji H, Li Y, Zhao X, Bai X, Fan X, Zhang F, Ruoff RS (2013) Nanoporous $Ni(OH)_2$ thin film on 3D ultrathin-graphite foam for asymmetric supercapacitor. ACS Nano 7:6237–6243

[7] Zhang LL, Zhao X (2009) Carbon-based materials as supercapacitor electrodes. Chem Soc Rev 38:2520–2531

[8] Zhang LL, Zhou R, Zhao X (2010) Graphene-based materials as supercapacitor electrodes. J Mater Chem 20:5983–5992

[9] Li H, Wu X, Zhou J, Liu Y, Huang M, Xing W, Yan Z, Zhuo S (2019) Enhanced supercapacitive performance of $MnCO_3$@rGO in an electrolyte with KI as additive. ChemElectroChem 6:316–319

[10] Wu ZS, Wang DW, Ren W, Zhao J, Zhou G, Li F, Cheng HM (2010) Anchoring hydrous RuO2 on graphene sheets for high-performance electrochemical capacitors. Adv Funct Mater 20:3595–3602

[11] Huang M, Zhao XL, Li F, Li W, Zhang B, Zhang YX (2015) Synthesis of Co_3O_4/SnO_2@MnO_2 core–shell nanostructures for high-performance supercapacitors. J Mater Chem A 3:12852–12857

[12] Huang M, Li F, Ji JY, Zhang YX, Zhao XL, Gao X (2014) Facile synthesis of single-crystalline NiO nanosheet arrays on Ni foam for high-performance supercapacitors. CrystEngComm 16:2878–2884

[13] Yao B, Chandrasekaran S, Zhang J, Xiao W, Qian F, Zhu C, Duoss EB, Spadaccini CM, Worsley MA, Li Y (2019) Efficient 3D printed pseudocapacitive electrodes with ultrahigh MnO_2 loading. Joule 3:459–470

[14] Xu W, Dai S, Liu G, Xi Y, Hu C, Wang X (2016) CuO nanoflowers growing on carbon fiber fabric for flexible high-performance supercapacitors. Electrochim Acta 203:1–8

[15] Huang M, Zhao XL, Li F, Zhang LL, Zhang YX (2015) Facile synthesis of ultrathin manganese dioxide nanosheets arrays on nickel foam as advanced binder-free supercapacitor electrodes. J Power Sources 277:36–43

[16] Huang M, Mi R, Liu H, Li F, Zhao XL, Zhang W, He SX, Zhang YX (2014) Layered manganese oxides-decorated and nickel foam-supported carbon nanotubes as advanced binder-free supercapacitor electrodes. J Power Sources 269:760–767

[17] Toupin M, Brousse T, Bélanger D (2004) Charge storage mechanism of MnO_2 electrode used in aqueous electrochemical capacitor. Chem Mater 16:3184–3190

[18] Huang Z-H, Song Y, Feng D-Y, Sun Z, Sun X, Liu X-X (2018) High mass loading MnO_2 with hierarchical nanostructures for supercapacitors. ACS Nano 12:3557–3567

[19] Li Q, Wang Z-L, Li G-R, Guo R, Ding L-X, Tong Y-X (2012) Design and synthesis of MnO_2/Mn/MnO_2 sandwich-structured nanotube arrays with high supercapacitive performance for electrochemical energy storage. Nano Lett 12:3803–3807

[20] Wu Z-S, Ren W, Wang D-W, Li F, Liu B, Cheng H-M (2010) High-energy MnO_2 nanowire/graphene and graphene asymmetric electrochemical capacitors. ACS Nano 4:5835–5842

[21] Li F, Xing Y, Huang M, Li KL, Yu TT, Zhang YX, Losic D (2015) MnO_2 nanostructures with three-dimensional (3D) morphology replicated from diatoms for high-performance supercapacitors. J Mater Chem A 3:7855–7861

[22] Le QJ, Huang M, Wang T, Liu XY, Sun L, Guo XL, Jiang DB, Wang J, Dong F, Zhang YX (2019) Biotemplate derived three dimensional nitrogen doped graphene@ MnO_2 as bifunctional material for supercapacitor and oxygen reduction reaction catalyst. J Colloid Interface Sci 544:155–163

[23] Qi H, Bo Z, Yang S, Duan L, Yang H, Yan J, Cen K, Ostrikov KK (2019) Hierarchical nanocarbon-MnO_2 electrodes for enhanced electrochemical capacitor performance. Energy Storage Mater 16:607–618

[24] Lv X, Zhang H, Wang F, Hu Z, Zhang Y, Zhang L, Xie R, Ji J (2018) Controllable synthesis of MnO_2 nanostructures anchored on graphite foam with different morphologies for a high-performance asymmetric supercapacitor. CrystEngComm 20:1690–1697

[25] Liu J, Jiang J, Bosman M, Fan HJ (2012) Three-dimensional tubular arrays of MnO_2–NiO nanoflakes with high areal pseudocapacitance. J Mater Chem 22:2419–2426

[26] Zhang X, Yu P, Zhang H, Zhang D, Sun X, Ma Y (2013) Rapid hydrothermal synthesis of hierarchical nanostructures assembled from ultrathin birnessite-type MnO_2 nanosheets for supercapacitor applications. Electrochim Acta 89:523–529

[27] Soriano L, Preda I, Gutiérrez A, Palacín S, Abbate M, Vollmer A (2007) Surface effects in the Ni2p x-ray photoemission spectra of NiO. Phys Rev B 75:233417

[28] Preda I, Gutiérrez A, Abbate M, Yubero F, Méndez J, Alvarez L, Soriano L (2008) Interface effects in the Ni2p x-ray photoelectron spectra of NiO thin films grown on oxide substrates. Phys Rev B 77:075411

[29] Chen J, Huang Y, Li C, Chen X, Zhang X (2016) Synthesis of NiO@MnO_2 core/shell nanocomposites for supercapacitor application. Appl Surf Sci 360:534–539

[30] Chao D, Zhou W, Ye C, Zhang Q, Chen Y, Gu L, Davey K, Qiao SZ (2019) An electrolytic Zn–MnO_2 battery for high-voltage and scalable energy storage. Angew Chem Int Ed 58:7823–7828

[31] Yu G, Hu L, Vosgueritchian M, Wang H, Xie X, McDonough JR, Cui X, Cui Y, Bao Z (2011) Solution-processed graphene/MnO_2 nanostructured textiles for high-performance electrochemical capacitors. Nano Lett 11:2905–2911

[32] Deng L, Zhu G, Wang J, Kang L, Liu Z-H, Yang Z, Wang Z (2011) Graphene–MnO_2 and graphene asymmetrical electrochemical capacitor with a high energy density in aqueous electrolyte. J Power Sources 196:10782–10787

[33] Zhang S, Yin B, Wang Z, Peter F (2016) Super long-life all solid-state asymmetric supercapacitor based on NiO nanosheets and α-Fe_2O_3 nanorods. Chem Eng J 306:193–203

[34] Xu W, Mu B, Wang A (2016) Facile fabrication of well-defined microtubular carbonized kapok fiber/NiO composites as electrode material for supercapacitor. Electrochim Acta 194:84–94